Development of ion-imprinted polymers for the selective extraction of Cu(II) ions in environmental waters

Pengchao Cao, Valérie Pichon, Catherine Dreanno, Kada Boukerma, Nathalie Delaunay

Development of ion-imprinted polymers for the selective extraction of Cu(II) ions in environmental waters

Pengchao Cao [a, b], Valerie Pichon [a, c], Catherine Dreanno [b], Kada Boukerma [b], Nathalie Delaunay [a]

[a] Department of Analytical, Bioanalytical Sciences, and Miniaturization, UMR 8231 Chemistry, Biology and Innovation, ESPCI Paris, PSL Research University, CNRS, 10 rue Vauquelin, 75005 Paris, France

[b] Laboratoire Détection, Capteurs et Mesures, Ifremer, Centre Bretagne, Technopole pointe du diable, 29280 Plouzané, France

[c] Sorbonne University, 75005 Paris, France

*Corresponding author: nathalie.delaunay@espci.fr (Nathalie Delaunay), tel: +33 140 794 651, Department of Analytical, Bioanalytical Sciences, and Miniaturization, UMR 8231 Chimie Biologie Innovation, CNRS, ESPCI Paris, PSL Research University, 75005 Paris, France.

Abstract

Several ion-imprinted polymers (IIPs) were synthesized via bulk polymerization with Cu(II) as template ion, methacrylic acid as functional monomer, ethylene glycol dimethacrylate as crosslinking agent, and azobisisobutyronitrile as initiator in acetonitrile or methanol as porogen solvent. Non-imprinted polymers (NIPs) were similarly synthesized but without Cu(II). After grounding and sieving, the template ions were removed from IIPs particles through several cycles of elimination in 3 M HCl. All NIPs were equally subjected to this acid treatment with the exception of one NIP, called unwashed NIP. The resulting IIP/NIP particles were packed in solid phase extraction (SPE) cartridges for characterization. The SPE protocol was designed by optimizing a washing step following the sample percolation to eliminate potential interfering ions prior to the elution of Cu(II), all fractions analyzed by inductively coupled plasma-mass spectrometry. The best IIP showed a high specificity (recovery of Cu(II) vs. interfering ions) and a good selectivity (retention on IIP vs. NIP). Its adsorption capacity was determined to be 63 μg g^{-1}. Then, a volume of 50 mL was percolated with 30 mg of IIP, thus giving rise to an enrichment factor of 24. Finally, applications to real samples (mineral and sea waters) were successfully performed. In addition, Brunauer-Emmett-Teller analyses showed that the surface area of the washed NIP was almost double that of the unwashed one (140.70 vs. 74.49 m^2 g^{-1}), demonstrating for the first time that the post-treatment of a NIP after its synthesis may have a significant impact on its porous structure, and thus need to be more precisely detailed by authors in the future papers.

Keywords: Ion-imprinted polymer; copper; solid-phase extraction; environmental water; ICP-MS.

Abbreviations

ACN: Acetonitrile; AIBN: Azo-N, N'-diisobutyronitrile; BET: Brunauer-Emmet-Teller; Bis-Tris: 2-[Bis(2-hydroxyethyl)amino]-2-(hydroxymethyl)propane-1,3-diol; dSPE: dispersive solid phase extraction; SPE: solid phase extraction; EGDMA: Ethylene glycol dimethacrylate; ICP-MS: Inductively coupled plasma mass spectrometry; IIP: Ion-

imprinted polymer; LOD: Limit of detection; LOQ: Limit of quantification; MAA: Methacrylic acid; NIP: Non-imprinted polymer.

1 Introduction

Copper, present in drinking, fresh and sea water, has an impact not only on the human health [1, 2] but also on marine ecosystems [3]. Currently, the determination of copper at trace-level can be carried out by various techniques, whereas the direct determination in real samples suffers from strong matrix interferences, especially with the most highly sensible techniques such as inductively coupled plasma mass spectrometry (ICP-MS) and electrothermal atomic absorption spectrometry [4]. For this reason, a sample treatment prior to the determination of Cu(II) is frequently required for the removal of matrix components or the enrichment of target analytes [5], and the most widely used technic is solid phase extraction (SPE). Its performance largely depends on the nature of the sorbent, whereas conventional sorbents like ion-exchange resins with or without the functionalization with metal-complexing agents lack selectivity. To address this drawback, ion-imprinted polymers (IIPs) which possess selective cavities for ions were first introduced by Nishide et al. in 1976 [6] and are of continuing interest up to now.

Synthesis of IIPs starts with the complexation between template ions and one or several appropriate functional monomers. After the copolymerization with a crosslinking agent, the resultant complexes are then immobilized in a highly cross-linked polymer matrix. Finally, template ions must be removed from the polymer so as to leave tailored cavities that are complementary to target ions in size and coordination geometries. This step is commonly performed using a strong acid from 0.1 M to 6.0 M as a leacher, such as HCl [7-9], HNO_3 [10-12] or H_2SO_4 [13-15], in order to disrupt the specific interactions between template ion and binding cavities. In order to evaluate the imprinting effect of IIP, a non-imprinted polymer (NIP) is synthesized as a control polymer by using the same conditions but without template ions. However, one point remaining unclear so far is whether the NIP should be subjected to the same treatment used to remove the template ions from the IIP, as no template ion was introduced for the NIP synthesis. To our knowledge, studies devoted to the influence of post-synthesis treatment of NIP have not yet been reported in the literature.

After synthesis, IIPs can be used in SPE with cartridge or in batch (so-called dispersive SPE, dSPE). dSPE is based on an adsorption equilibrium between sorbent particles and analytes under stirring for a sufficiently long incubation time. In practice, a follow-up operation of filtration, centrifugation, or decantation is necessary to recover the subsequent solution for its analysis, which is time consuming and labor intensive. By contrast, SPE with a cartridge offers many advantages since particles are immobilized allowing the direct and rapid percolation of samples and recovery of solutions. Thanks to that convenience and simplicity, one or several washing steps can be applied to eliminate potential interfering ions before the final elution of target ions.

Nowadays many studies have been reported on the preparation of IIPs dedicated to Cu(II) [16]. However, almost all of those IIPs were used in dSPE rather than SPE. To the best of our knowledge, there are only five papers on Cu(II)-targeting IIPs in SPE including selectivity study [17-21] and two of them did not validate their analytical methods with real samples [18, 19]. Moreover, none of them implemented an optimized washing step, to eliminate interfering ions and thus optimizing the specificity, which is considered as one of the fundamental advantages of SPE as described previously.

In this work, Cu(II), methacrylic acid (MAA), ethylene glycol dimethylacrylate (EGDMA), and azo-N, N'-diisobutyronitrile (AIBN) were selected as template ion, ligand, crosslinking agent, and initiator, respectively. Methanol and acetonitrile (ACN) were tested as porogen solvent. Several IIPs were synthesized via bulk polymerization by varying the nature and volume of porogen solvent as well as the time of complexation between Cu(II) and MAA. After grounding and sieving, the template ions were removed by washing IIP particles with 3 M HCl. All related NIPs were subjected to the same acid treatment for being rigorous references, while one NIP remained unwashed for investigating the effect of acid treatment. The resulting IIPs/NIPs were characterized in SPE cartridges by involving a washing step following the sample percolation prior to the elution of Cu(II) ions. Using ICP-MS for the analysis of the different resulting SPE fractions, each SPE step was optimized for promoting selectivity (retention on IIP *vs.* NIP) and specificity (recovery of target ion *vs.* interfering ions). The most promising IIP was thereupon selected. Its capacity, breakthrough volume, and enrichment factor were

determined under the optimum SPE conditions. Finally, applicability to real samples (i.e. mineral and sea waters) as well as reusability were assessed.

2 Material and methods

2.1 Reagents

$Cu(NO_3)_2$ (99.999%), EGDMA (98%), MAA (99%), and NaOH (98%) were purchased from Sigma-Aldrich (St Quentin Fallavier, France). AIBN was obtained from Acros Organics (Noisy-le-Grand, France). HPLC-grade acetonitrile and HPLC-grade methanol were purchased from Carlo Erba-Réactifs-SDS (Val De Reuil, France). Water used throughout this work was purified by a Milli-Q purification system from Millipore (Molsheim, France) and was of ultra-pure grade. 37% (wt.%) hydrochloric acid (Emsure, Merck) was diluted to 3 M for the removal of template ions. EGDMA and MAA were distilled prior to use according to a protocol reported in our previous study in order to remove inhibitors [9]. All other reagents were used as received.

Standard mono-elemental ICP solutions of Co(II), Ni(II), Cu(II), and Zn(II) at 1 g L^{-1} were purchased from Sigma-Aldrich. Calibration solutions were prepared through serial dilutions of the standard solutions with 2% (wt.%) HNO_3 which is obtained by diluting 65% (wt.%) HNO_3 from Merck (Darmstadt, Germany). A tuning solution for ICP-MS from Agilent Technologies (Les Ulis, France) containing Ce, Co, Li, Mg, Tl, and Y at 1 mg L^{-1} in 2% (wt.%) HNO_3 was also used. Multi-elemental solution for SPE experiments at 30 µg L^{-1} containing Co(II), Ni(II), Cu(II), and Zn(II), as well as mono-elemental solution of Cu(II) at different concentrations, were prepared through appropriate dilutions of the standard solutions with water. The pH was adjusted with HNO_3 or NaOH.

2.2 Synthesis of the IIPs

Firstly, 0.5 mmol of Cu(II) as template ion was dissolved in a certain volume of porogen solvent (see **Table 1**). Then 2 mmol of functional monomer MAA was immediately added. The mixture was placed under continuous magnetic stirring for the complexation between Cu(II) and MAA. Thereafter, 10 mmol of EGDMA as crosslinking agent and 0.12 mmol of AIBN as initiator were sequentially added to the solution. The vial containing the polymerization mixture was placed in an ice bath and meanwhile purged

with N_2 for 15 min to remove oxygen which may inhibit radical polymerization. At last, the vial was sealed and immersed in a water bath at 60 °C for 24 h in order to perform the polymerization. In parallel with each IIP, a NIP was synthesized under the same conditions but without the addition of Cu(II).

After polymerization, the IIPs and the NIPs were grounded and sieved with a grinder MM 301 and a vibratory sieve shaker AS 200 both from Retsch (Eragny sur Oise, France). Afterwards, polymer particles between 25 and 36 μm were collected for further use. For template removal, all IIP particles were placed in 3 M HCl under stirring for 5 or 7 cycles of 20 h. All NIP particles were subjected to the same acid treatment as their IIP except one NIP (hereinafter called unwashed NIP). Nevertheless, a part of the unwashed NIP particles was submitted to 3 cycles of stirring in 3 M HCl that was only used for the determination of surface area. The resultant supernatant of every cycle was collected through filtration and then assayed by ICP-MS to follow the completion of template removal. Next, the IIP/NIP particles were rinsed with water for the neutralization, and then sedimented in MeOH/water (4/1, v/v) to eliminate the residual fine particles. After being dried at 50 °C, each accurately weighted polymer (30 mg) was packed between two polyethylene frits (20 μm porosity, Merck) into a 1 mL polypropylene cartridge (Merck).

Table 1. Synthesis conditions of IIPs with 0.5 mmol of Cu(II), 2 mmol of MAA, and 10 mmol of EGDMA as template ion, ligand, and crosslinking agent, respectively. Synthesis of the corresponding NIPs: same conditions except the addition of Cu(II) as template ion, plus the indication of the application or not to the NIP of the acid treatment step used to remove the template ions from IIPs after their synthesis.

Polymer	Porogen solvent	Volume of porogen solvent	Time of complexation between Cu(II) and MAA	Acid treatment for its NIP
IIP-M	Methanol	3 mL	2 h	Yes
IIP-3	ACN	3 mL		Yes
IIP-2		2 mL		Yes
IIP-1		1 mL		Yes
IIP-1’				No
IIP-1(3d)			3 days	Yes

2.3 ICP-MS conditions

Determination of elements was performed by means of an Agilent 7850 ICP-MS equipped with a quartz concentric nebulizer, a quartz Scott spray chamber, a quadrupole analyzer, and an Agilent ASX-500 autosampler. Acquisition and analysis parameters are listed in **Table S1** in Supplementary Material. Prior to each batch of measurements, an Agilent tuning solution for performance check was utilized to ensure sensitivity, stability (RSD < 3%), oxide less than 0.65%, and double-charged ion less than 1.5%. Limit of detection (LOD) and limit of quantification (LOQ) of tested elements were calculated as follows:

$$LOD = 3\sigma/k \quad \text{Eq. (1)}$$

$$LOQ = 10\sigma/k \quad \text{Eq. (2)}$$

where σ is the standard deviation of counts per second (cps) of 10 blank solutions (i.e. 2% (wt.%) HNO_3), and k is the sensitivity of the instrument (cps/(ng L^{-1})) for tested element. The LODs and LOQs obtained in 2% HNO_3 are provided in **Table S2** in Supplementary Material.

2.4 SPE procedure and its optimization

Prior to use, IIP/NIP cartridges were conditioned with 3 mL of HNO_3 solution at pH 5.5. A sample containing an appropriate amount of Cu(II) with or without interfering ions was next percolated. The following washing step was optimized testing a series of HNO_3 solutions at decreasing pH from 5.0 to 1.0, and finally performed with the most promising pH as well as an appropriate volume. Finally, elution was carried out with 2 mL of 5% HNO_3. A flow rate of 1 mL min^{-1} was used for each SPE step. The SPE fractions were collected in metal-free tubes for their analysis in ICP-MS. After each use, the cartridges were washed with water to neutralization and stored at room temperature. The enrichment factor was calculated as the ratio of the percolated sample volume to the elution fraction volume (2 mL) multiplied by the recovery of analyte.

2.5 Brunauer–Emmett–Teller (BET) surface area analysis

For BET analysis, 100 mg of IIP and NIP were introduced in the sample holder which is composed of a glass rod and a glass tube of 9 mm with a bulb. Next, the sample was

degassed under vacuum at 180 °C for 6 h through a VacPrep 061 sample degas system (Micromeritics®, Merignac, France). The temperature for degassing (i.e. 180 °C) was predetermined according to a preliminary study by thermogravimetric analysis (TGA) (see **Figure S1** in Supplementary Material). After degassing, the sampling tubes were reweighted for the final calculation of surface area. At last, nitrogen adsorption-desorption isotherms at -196 °C were obtained using a TriStar II PLUS apparatus (Micromeritics®, Merignac, France). Based on the amount of N_2 adsorbed at pressures $0.04 < P/P_0 < 0.3$, the surface area was calculated with the application of BET model [22].

2.6 Adsorption isotherms modeling

Adsorption isotherm models in dSPE used classically C_e as equilibrium concentration and Q_e as adsorption capacity at equilibrium. Given that adsorption data were obtained in SPE with cartridge in the present work, judicious adaptions were made for the definition of those two parameters using the following equations:

$$C_e = (m_i - m_E)/V \qquad \text{Eq.(1)}$$

$$Q_e = m_E/m_s \qquad \text{Eq.(2)}$$

where m_i is the initial amount of analyte in the percolated sample (mg), m_E is the recovered amount of analyte in the elution fraction (mg), V is the volume of the percolated sample (L), and m_s is the quantity of sorbent (g).

Seven isotherm models were investigated: Langmuir, Freundlich, Redlich–Peterson, Sips, Dubinin-Radushkevich, Scatchard (single-site), and Scatchard (dual-site). Each isotherm fitting was performed by means of Origin (OriginLab Corporation).

2.7 Real sample pretreatment

Two commercial mineral waters of Mont Roucous® and Evian® were selected. Natural sea water was collected at Sainte Anne du Portzic (48°21'N, 4°33'W; Brittany, France) in high-density polyethylene bottles. The salinity of the sea water was measured using Marel Iroise buoy [23]. Each non-spiked water was subjected to the developed SPE procedure and ICP-MS analysis. Then, the initial content of Cu(II) was evaluated by taking into account the recovery of Cu(II) previously determined in ultra-pure water, for the same percolated volume. The two mineral waters were accurately spiked with Cu(II)

at 4 µg L^{-1}, while the sea water at 2, 4, and 6 µg L^{-1}. All samples were adjusted at pH 5.5 with HNO_3. For mineral waters, 50 mL of the non-spiked or spiked samples were percolated, followed by a washing step with 5 mL of HNO_3 at pH 4. The elution was performed with 2 mL of 5% HNO_3. For sea water, 1 mL of the non-spiked or spiked samples were percolated, followed by the same washing step as mentioned above. The elution was performed with 1 mL of 5% HNO_3.

3 Results and discussion

3.1 Synthesis of the IIPs and the NIPs

For the synthesis of an IIP, substantial components include template ion, functional monomer(s), crosslinking agent, initiator, and porogen solvent. According to our literature review for the past two decades, Cu(II) was always used as template ion while functional monomers can be categorized into two general groups, i.e. vinylated ligands and non-vinylated ligands. MAA is considered as one of the most typical and frequently used vinylated ligands since it was used for the IIP preparation not only for Cu(II) [24-26], but also for other elements such as Ni, Zn, Cd, Hg, Ag, Pb, As, Cr, and Ln [16, 27]. Regarding non-vinylated ligands used for the synthesis of IIP for Cu(II), a large variety is found in the literature such as thiosemicarbazide [24], salen [28], aniline [29], etc. However, it was demonstrated in our previous work [9] that non-vinylated ligands can leak out from IIPs during template ion removal and SPE use since they are just trapped inside the polymer network. Vinylated ligands were thus preferred in this work. EGDMA and AIBN are found to be the most common crosslinking agent and initiator, respectively [16]. Regarding porogen solvent for the IIP synthesis with Cu(II), methanol seemed more used than ACN, ethanol, dimethyl sulfoxide or dimethylformamide [30].

According the aforementioned, in this work, Cu(II), MAA, EGDMA, methanol or ACN, and AIBN were selected as template ion, ligand, crosslinking agent, solvent, and initiator, respectively. Since the complex $Cu(MAA)_2$ was reported in many studies [18, 19, 31, 32], the molar ratio of Cu(II)/MAA was fixed at 1/4 to favor the complexation. As shown in **Table 1**, five synthesis conditions were studied by varying the nature of porogen solvent (i.e. methanol or ACN), the volume of porogen solvent (i.e. 3 mL, 2 mL, or 1 mL), and finally the time of complexation between Cu(II) and MAA (i.e. 2 h or 3 days). Among

them, IIP-1' was obtained repeating the synthesis conditions of IIP-1. Regarding the NIPs, each one was synthesized with the conditions of its IIP but in the absence of the template ions Cu(II).

For template ion removal, all IIP particles were placed in 3 M HCl under stirring for 5 or 7 cycles of 20 h. All NIP particles were subjected to the same acid treatment except one NIP (hereinafter called unwashed NIP). The leached Cu(II) during the template removal was quantified by analyzing the supernatant of each cycle by ICP-MS. For all the NIPs, no Cu(II) was detected in any collected supernatant as expected. For the IIPs, percentages of leached Cu(II) in each cycle were calculated as compared to the amount of Cu(II) introduced initially for their synthesis (see **Table 2).** Nearly all Cu(II) was readily leached from IIPs during the first three cycles. Nonetheless, supplementary cycles were necessary to remove the residual Cu(II) in trace amounts, which may otherwise leak from the IIPs and threaten to contaminate samples during their forthcoming SPE use. Indeed, even if the percentages of leached Cu(II) starting from the 4^{th} cycle seem minuscule (i.e. < 2%), they were actually non-negligible as compared to the trace amount of Cu(II) targeted in environmental waters with an order of magnitude of several µg L^{-1}. In the case of IIP-1(3d), the residual Cu(II) in trace amount was still present after the 5^{th} cycle. Therefore, additional cycles (i.e. 6^{th} and 7^{th} cycles) were conducted for this IIP-1(3d). Overall, for all IIPs, the sums of percentages confirmed the completion of template removal. The IIPs were therefore considered ready for their characterization in SPE. It worth noting that the small overestimation of total recovery was related to the incomplete recuperation of IIP particles during the filtration step, after each cycle.

Table 2. Percentage of leached template Cu(II) ions (as compared to the amount of Cu(II) introduced initially for the IIP synthesis) during the template removal in each cycle (stirring in 3 M HCl, 20 h).

Cycle	IIP-M	IIP-3	IIP-2	IIP-1	IIP-1'	IIP-1(3d)
1	88%	90%	100%	78%	90%	87%
2	14%	14%	14%	22%	16%	11%
3	2%	3%	2%	6%	5%	2%
4	0.25%	1.20%	0.61%	1.12%	0.14%	0.65%
5	0.01%	1.20%	0.31%	1.40%	0.05%	0.20%
6	Not performed					0.15%
7						0.06%
Sum	104%	109%	117%	108%	111%	101%

3.2 Determination of percolation and elution conditions of the SPE protocol

After the template ion removal step, 30 mg of each polymer particles were packed in a given SPE cartridge and the SPE protocol was next optimized. In principle, an SPE protocol is composed of three successive steps: the sample percolation where the targeted ions are expected to be retained by the sorbent, washing to eliminate interfering ions that could be retained on the sorbent by non-specific interactions, and elution of the targeted ions. Regarding the percolation condition, the influence of medium on the retention of ions on polymers was investigated. Two different percolation media were prepared: a 25 mM Bis-Tris buffer and ultra-pure water, both spiked at 30 μg L^{-1} with Cu(II) and adjusted at pH 6.0. In ultra-pure water, Cu(II) ions were entirely retained by the tested polymers (IIP-1, 2, and 3) whereas > 85% of loss was found in Bis-Tris buffer. The retention of Cu(II) ions appeared to be significantly reduced in a Bis-Tris buffer, even if the buffer concentration was low. This is very likely because Cu(II) was strongly complexed by Bis-Tris to the extent that the sorbents hardly predominated the adsorption competition. Indeed, this phenomenon that a buffer could reduce the retention of Cu(II) on sorbents was already reported in literature [33, 34]. This is why non-buffered media (i.e. ultra-pure water with a pH adjusted with HNO_3) is herein suggested as a preferable option to avoid the aforementioned problem. Moreover, the pH for percolation of samples was slightly reduced from 6.0 to 5.5, which did not impact the retention of Cu(II) ions but allowed a better accuracy of experimental results since Cu(II) is known to start to precipitate as $Cu(OH)_2$ above pH 6 [35].

Elution condition was next investigated. This step consists in desorbing the retained ions and also allowing the regeneration of sorbents. Similar to the principle of template removal, strong acids like HNO_3 and HCl as well as chelating agents are commonly used as eluents. In this work, Cu(II) was efficiently eluted from all studied IIPs within 2 mL of 5% HNO_3, HNO_3 being preferred because it gives fewer matrix effects than HCl or chelating agents for the subsequent analysis by ICP-MS.

3.3 Specificity and selectivity of the IIP synthesized in methanol

The percolation and elution media previously determined (i.e. non-buffered media at pH 5.5 and 2 mL of 5% HNO_3, respectively) were used for the characterization of the IIP-M. Without carrying out a washing step, Cu(II) ions but also the tested interfering ions Co(II), Ni(II), and Zn(II), selected as they have very close physico-chemical properties and ionic radii [36], were all retained during the percolation and eluted during the elution. It means that no specificity was observed between the target Cu(II) ions and the other tested interfering ions. Moreover, all the ions were retained on the IIP-M but equally on its NIP, demonstrating a lack of selectivity of the IIP-M in comparison with its NIP. This is why the optimization of a washing step was mandatory.

In practice, the purpose was to find an optimum washing force that is strong enough to disrupt the so-called non-specific interactions occurring at the polymer surface, as it is the case on the NIP, while maintaining the more numerous and/or stronger interactions occurring inside the imprinted cavities of the IIP, so-called the specific ones. In this work, the adjustment of the washing force was carried out by adjusting the pH of the washing solutions, because the pH value influences significantly the adsorption/desorption of ions by affecting deprotonation/protonation of the polymerized functional monomer (i.e. MAA, pK_a 6.4 - 6.5 when incorporated in a polymer matrix [37, 38]) and/or the number of H^+ ions as competitive eluent ions. In addition to pH, the volume of washing solutions plays also a role in the desorption of ions.

In the first tested SPE protocol, the washing steps were implemented with a series of 0.5 mL of HNO_3 solutions at pH 5, 4, 3, 2, and 1. As can be observed in **Figure 1a**, all ions were strongly retained on IIP-M and NIP-M until the second washing step (W2) at pH 4, and then were eluted almost together at the third washing step (W3) at pH 3. This means that the pH 4 was too weak to eliminate interfering ions, whereas the pH 3 was too strong for retaining target ions Cu(II). In view of that, a second SPE protocol was conducted using a series of washing solutions at pH values between 4 and 3 (i.e. 3.8, 3.6, 3.4, 3.2, and 3.0). As a result, nearly all ions retained on NIP-M were successfully eliminated at pH 3.6 (W2) whereas they remained well retained on IIP-M (**Figure 1b**), showing a selectivity between the IIP-M and its NIP. Moreover, some specificity between the target Cu(II) ions and the interfering ions can be observed, as a higher percentage of Cu(II) was

determined in the W4 fraction. Nevertheless, a lot of Cu(II) was eliminated in the W3 fraction at pH 3.4. This is why a higher pH value of 3.6 was selected as the most appropriate washing pH, and the washing volume was next varied. The final SPE protocol was performed with 5 x 0.5 ml of HNO_3 solutions at pH 3.6 for the washing step. As expected, the ions retained on NIP-M were firstly eluted at W1 and W2 confirming the high selectivity of IIP-M, and then the ions retained on IIP-M were progressively eluted step by step from W3 to the elution step (**Figure 1c**). However, the retention of Cu(II) on IIP-M was only slightly stronger than that of interfering ions, which signified a poor specificity of IIP-M towards Cu(II).

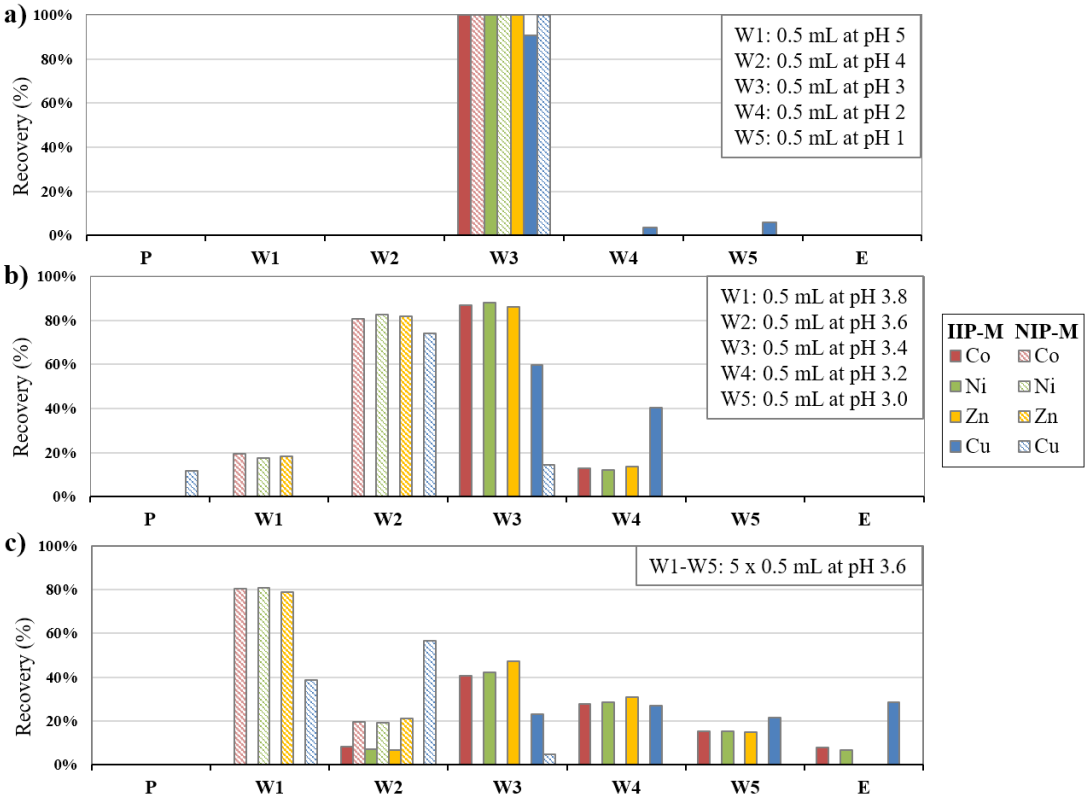

Figure 1. SPE profiles of Co(II), Ni(II), Zn(II), and Cu(II) on IIP-M and its NIP. Percolation (P): 1 mL of HNO_3 solution at pH 5.5 spiked with Co(II), Ni(II), Zn(II), and Cu(II) at 30 µg L^{-1} for each; Washing (W1-W5): a) 5 x 0.5 mL of HNO_3 at pH 5, 4, 3, 2, and 1. b) 5 x 0.5 mL of HNO_3 at pH 3.8, 3.6, 3.4, 3.2 and 3.0. c) 5 x 0.5 mL of HNO_3 at pH 3.6; Elution (E): 2 mL of 5% HNO_3.

Furthermore, it is worthwhile to notice in **Figure 1c** that at W2, the recovery of Cu(II) on the NIP-M is much higher than that of the interfering ions. This observation could be

explained by the Irving-Williams order pertaining to the stability of transition-metal complexes [39]. Indeed, Cu(II) was found to have the highest metal complex stability over Co(II), Ni(II), and Zn(II) irrespective of the nature of the coordinated ligand. Due to this reason, the NIP-M possesses an intrinsic affinity towards Cu(II) though the ligand MAA was disorderly distributed inside its network without forming specific cavities. As a matter of fact, many NIPs in the literature showed results consistent with the Irving-Williams order in spite of extremely distinct functional monomers employed for their synthesis, but their intrinsic affinity towards Cu(II) is usually not discussed. **Table S3** in Supplementary Material listed some of those NIPs described in publications dealing with IIPs targeting Cu(II) and where the polymer evaluation was carried out with similar ions to the ones used here, i.e. Cu(II), Co(II), Ni(II), and Zn(II). Those NIPs showed a higher affinity for Cu(II) than for Co(II), Ni(II), and Zn(II).

3.4 Optimization of IIPs synthesized in ACN and characterization

By considering the poor specificity towards Cu(II) observed previously with IIP-M, a less polar and aprotic porogen solvent, ACN was employed as the alternative to methanol. Indeed, it is generally accepted that porogen solvent plays a pivotal role in the synthesis of IIPs since it is required to enable the solubility of all reactants, then promote the stability of complexes between template ions and functional monomers, and finally generate the porous structure during polymerization.

3.4.1 Optimization of the amount of ACN used in the IIP synthesis

Three IIPs, i.e. IIP-3, IIP-2, and IIP-1, were synthesized with 3, 2, and 1 mL of ACN, respectively, for 0.5 mmol of Cu(II). The retention of ions of interest on these IIPs was assessed by percolating them at 40 µg L^{-1} in 1 mL of a HNO_3 solution at pH 4.4. This pH value was selected to weaken the retention of ions on IIPs and thus facilitate their comparison. As illustrated in **Figure S2** in Supplementary Material, different quantities of ions were lost during the percolation, but with various degrees as expected. Among the three IIPs, IIP-1 exhibited the best retention of the tested ions, especially the ion of interest Cu(II). This may result from the fact that the complexation between the template ions and MAA monomers was carried out in a most concentrated medium in the case of

IIP-1 (1 mL) as compared with IIP-2 and IIP-3 (2 mL and 3 mL, respectively), favoring the formation of specific cavities. The IIP-1 was therefore selected for further studies.

3.4.2 Study of repeatability, specificity and selectivity of IIP-1

According to the aforementioned methodology illustrated with IIP-M, the optimization of the washing step was performed for IIP-1 in a similar way, with percolation and elution steps conducted under the predetermined conditions in section 3.2. Regarding specificity, first good results were obtained by applying a washing with 5 x 0.5 mL of HNO_3 at pH 4.0, which allowed to remove most of the interfering ions (i.e. Co(II), Ni(II), and Zn(II)) from IIP-1. Therefore, in the elution fraction, the recovery of Cu(II) was much higher than those of the interfering ions, resulting in a remarkable specificity of the IIP-1 towards Cu(II) (**Figure 2**a). To assess the synthesis repeatability, an IIP-1', prepared under the same synthesis conditions as IIP-1 but on a different day, was subjected to the same SPE protocol. It can be clearly seen that the IIP-1' presented highly similar SPE profiles to those on IIP-1. Moreover, the same SPE protocol was repeated 3 times for each IIP, showing low RSD values on the recoveries ($\leq$ 5%). Those results demonstrated therefore an excellent repeatability not only of the developed SPE protocol, but also of the IIP synthesis which is meanwhile a feature barely studied in the literature.

Regarding selectivity, the recoveries in each fraction of IIP-1 or 1' have to be compared to the ones obtained with the two kinds of corresponding NIPs, a wash and an unwashed NIP. As displayed in **Figure 2**b, a considerable discrepancy can be observed by comparing the SPE profiles obtained on the two NIPs. In the case of NIP-1, most interfering ions with only a little portion of Cu(II) were eliminated during the 5 fractions of washing, leading to a high recovery of Cu(II) over other ions in the elution fraction. This affinity of NIP-1 towards Cu(II) can be ascribed to the same reason related to the Irving-Williams order as described previously. By contrast, in the case of unwashed NIP-1, practically all the ions including Cu(II) were found to be eliminated during only the first two fractions of washing (W1+W2), leaving finally a tiny recovery of Cu(II) (i.e. 10 $\pm$ 3%) in the elution fraction. The retention of ions on unwashed NIP seemed significantly reduced without the acid treatment for its preparation. Under those SPE conditions, IIP-1 presented an excellent selectivity relative to unwashed NIP-1, but no

obvious selectivity relative to NIP-1. To further investigate the latter, another SPE protocol was conducted by doubling the volume of previous washing solution with the use of 5 x 1 mL of HNO_3 at pH 4.0. Consequently, as indicated in **Figure 2**c, a weak selectivity relative to NIP-1 can admittedly be observed but at the expense of a reduced and low recovery of Cu(II) (i.e. IIP-1 *vs.* NIP-1: 51 ± 4% *vs.* 26 ± 3%).

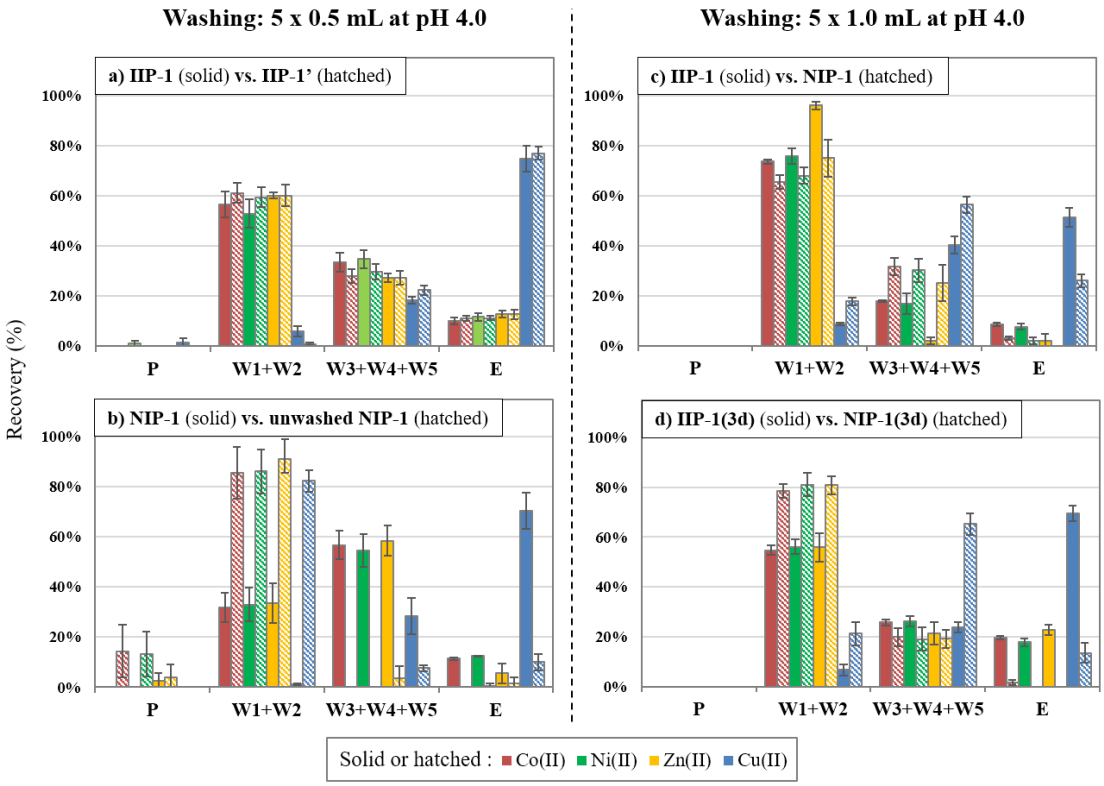

Figure 2. SPE profiles of Co(II), Ni(II), Zn(II), and Cu(II) obtained using a washing step (W1-W5) of 5 x 0.5 mL of HNO_3 at pH 4 **a)** on IIP-1 and IIP-1', **b)** NIP-1 and unwashed NIP-1, and a washing step (W1-5) of 5 x 1 mL of HNO_3 at pH 4 **c)** on IIP-1 and NIP-1, **d)** on IIP-1(3d) and NIP-1(3d). Percolation (P): 1 mL of HNO_3 at pH 5.5 spiked with Co(II), Ni(II), Zn(II), and Cu(II) at 30 µg L^{-1} for each; Elution (E): 2 mL of 5% HNO_3. All experiments were conducted in triplicate (n = 3) and the results were averaged.

To better understand the different behaviors of NIP-1 and unwashed NIP-1, nitrogen adsorption/desorption experiments were implemented for the determination of surface area. Note that NIP-1 underwent the same 5 cycles of stirring in 3 M HCl as IIP-1 and 1', which correspond to the process of template removal after polymerization. As presented in **Table 3**, the unwashed NIP-1 possesses a surface area roughly twice as small as that of

NIP-1 (74.49 ± 0.35 *vs.* 140.70 ± 0.05 $m^2 g^{-1}$, respectively). That explains clearly why the retention of ions on unwashed NIP was much lower than that on NIP-1 during SPE, even though the retention of ions derived from the same non-specific interactions in both cases. To confirm this tendency, a part of the unwashed NIP particles was submitted to 3 cycles of stirring in 3 M HCl (so-called intermediary NIP-1) and their surface area was measured (**Table 3**). The surface area of the NIP particles was found to increase continuingly as the number of cycles of acid treatment went from 0 to 3, and 5. The possible explanation is that the strong acidic conditions may break up the polymer backbone, leading to a less cross-linked and more porous structure. This phenomenon, in the present work, influenced significantly the physicochemical properties of NIP-1, which then exerted a decisive impact on the selectivity evaluation for IIP-1. However, it must be pointed out that the post-treatment of NIP after its polymerization is hardly ever specified in the literature. It is only well established concerning its synthesis, that a NIP should be synthesized in the same conditions as its corresponding IIP except without template ion. Therefore, this study revealed for the first time that the post-treatment of NIP needs close heed since its influence may not be neglected, and thus need to be specified.

Table 3. BET surface area values of IIPs/NIPs synthesized using 2 mmol of MAA, 10 mmol of EGDMA in 1 mL of ACN with/without 0.5 mmol of Cu(II) after different cycles of stirring in HCl 3 M. Each cycle lasted 20 h.

Polymer	Cycles of stirring in HCl 3 M	BET surface area ($m^2 g^{-1}$)
Unwashed NIP-1	0	74.49 ± 0.35
Intermediary NIP-1	3	134.72 ± 1.22
NIP-1	5	140.70 ± 0.05
NIP-1(3d)	7	144.47 ± 0.66
IIP-1	5	< 3
IIP-1’	5	
IIP-1(3d)	7	

In addition, IIP-1 and IIP-1’ were also submitted to the nitrogen adsorption/desorption experiments. Unfortunately, the amount of adsorbed nitrogen was inferior to the LOD of the apparatus whereby their surface areas were calculated to be inferior to 3 $m^2 g^{-1}$. Even though this value seemed relatively small, IIP-1 and IIP-1’ exhibited practically stronger retention of Cu(II) ions than the washed or unwashed NIP-1 of greater surface areas. This

undoubtedly corroborates the formation of specific cavities inside the IIP network, which is in satisfactory agreement with the principle and objective of our synthesis. Besides, in literature, the IIP surface area values were reported to range from several hundreds [8, 40-43] to a few [44-48] of m^2 g^{-1}, or even less than 1 m^2 g^{-1} [25]. However, these results suggest meanwhile that IIP-1 and IIP-1' have a quite different structure than both kinds of NIP. Moreover, similar case can also be found in literature that an IIP presented lower surface area than the corresponding NIP [45, 49, 50]. This constitutes a problem since an ideal control polymer is supposed to have a similar or comparable structure, which is here neither the case of unwashed NIP nor the case of washed NIP. Further, the unwashed NIP-1, although imperfect, might be a more appropriate control polymer than the washed one since it has a closer surface area to IIP-1, and it led indeed to a better selectivity. On this issue, an alternative control polymer to NIP can be considered by using an IIP synthesized with an element different from Cu(II), insofar that this synthesized IIP would more likely have a structure similar to Cu-IIP than a NIP. The feasibility of this strategy has recently and for the first time been studied in another study by our group [50].

3.4.3 Effect of the complexation time

In order to enhance the retention on IIP-1 and its selectivity (see **Figure 2**c), the effect of complexation time was studied. The protocol used to synthesize the IIP-1 was selected but by increasing the complexation time from 2 h to 3 days, which led to an IIP called IIP-1(3d). Under the same SPE conditions, IIP-1(3d) gave rise to a higher recovery of Cu(II) in the elution fraction, i.e. 70 ± 3%, as compared to 51 ± 4% in the case of IIP-1 (**Figure 2**). Thanks to that, a good selectivity of IIP-1(3d) relative to its NIP(3d) was obtained as well, even though the NIP-1(3d) underwent the same acid treatment and has a much higher surface area (see **Table 3**). It seems that a stronger imprinting effect of template ion was obtained by applying a longer complexation time. Moreover, IIP-1(3d) presented a high specificity towards Cu(II) with respect to the interfering ions Co(II), Ni(II), and Zn(II), which is close to the specificity previously observed with IIP-1 or IIP-1' (**Figure 2**a). In order to compare these results with the ones previously published in literature of IIPs targeting Cu(II) and based on MAA, it appears that only one study evaluated specificity and selectivity with a SPE procedure carried out in a column and

calculation of extraction recoveries [17]. In this study, the specificity seems low: extraction recoveries between 91 and 100% for Cu(II) vs. 86 and 99% for Zn(II), Co(II), and Ni(II) for concentrations between 0.1 and 1 mg L^{-1} of binary mixtures of Cu(II) and the tested interfering ion. Differences in extraction recoveries between Cu(II) and interfering ions were only observed at a concentration of 5 mg L^{-1} (between 95 and 100% for Cu(II) vs. 52% for Co(II), 66% for Ni(II) and 83% for Zn(II)), i.e. with tested amounts close to the capacity, for which specificity cannot be accurately evaluated. Regarding selectivity, it was also not demonstrated as extraction recoveries of Cu(II) varied between 91 and 100% on the IIP vs. 87 and 100% on the NIP. This may be due to the lack of use of a washing step, between percolation and elution. Since IIP-1(3d) was identified as the most promising sorbent in this work, it was subjected to further characterizations.

3.5 Capacity study and isotherm modeling

In parallel to specificity and selectivity, adsorption capacity is another essential feature of IIPs. It is expressed as the maximum amount of adsorbed analytes per gram of IIP. As IIP-1(3d) appeared as the most promising sorbent, its capacity was determined by assessing the extraction recoveries when percolating an increasing amount of Cu(II) in 1 mL of HNO_3 at pH 5.5. It is worth mentioning that the optimum washing step (i.e. 5 x 1 mL of HNO_3 at pH 4) was involved before the elution step to ensure a specific retention on the IIP-1(3d), thereby allowing the measure of the capacity provided only by specific cavities and not by additional non-specific interactions.

Figure 3 presents the plot between the recovered amount of Cu(II) in the elution fraction against the initial amount of Cu(II) introduced during percolation. As displayed, two different slopes (steep solid one and gentle dotted one) can be observed with the IIP-1(3d) while one single gentle slope with its NIP. The first slope of IIP-1(3d) steeper than that of its NIP corresponds to a better recovery of Cu(II), reflecting the retention of Cu(II) by specific interactions. As the amount of percolated Cu(II) increases, the specific cavities of IIP-1(3d) were saturated so that Cu(II) started to be retained by non-specific interactions. This is why the slope of its NIP curve was used to draw the dotted line of the IIP-1(3d) at higher concentrations, as it was already done in literature [51], where only non-specific

interactions were supposed to occur. It worth noting that the Cu(II) amount retained by these non-specific interactions should not be taken into account for evaluating the specific binding capacity. Given this, the point of intersection of the two IIP-1(3d)'s linear curves is referred as its adsorption capacity, estimated to be 63 μg g^{-1}.

Admittedly, this capacity value seems in the bottom bracket among other Cu-IIPs' capacities reported in literature, which is likely due to its limited surface area. However, it must be pointed out that quite many capacities of the same order of magnitude as μg g^{-1} have already been reported mainly with IIPs targeting other heavy metals or metalloids [26, 52-59]. Moreover, an adsorption capacity as 63 μg g^{-1} is more than sufficient to extract traces of Cu(II) from environmental water samples. On the other hand, most characterizations in literature were carried out in dSPE generally without using a washing step. In such case, the adsorption capacity is prone to be overstated because non-specific interactions may contribute to the uptake of analytes. To prove more visually the effect of washing step on the capacity determination, similar experiments as above were carried out on IIP-1(3d) and its NIP but by skipping the washing step. With this approach, the maximum amount of Cu(II) retained by IIP-1(3d) was observed to be nearly four times higher than the amount obtained with the washing step (see **Figure S3** in Supplementary Material). Besides, the NIP-1(3d) presented a retention of Cu(II) paradoxically better than the IIP-1(3d), which is very probably due to a higher surface area and thus more numerous and accessible non-specific sites. Hence, these data are apparently not reliable for the determination of adsorption capacity, demonstrating the vital role of the washing step.

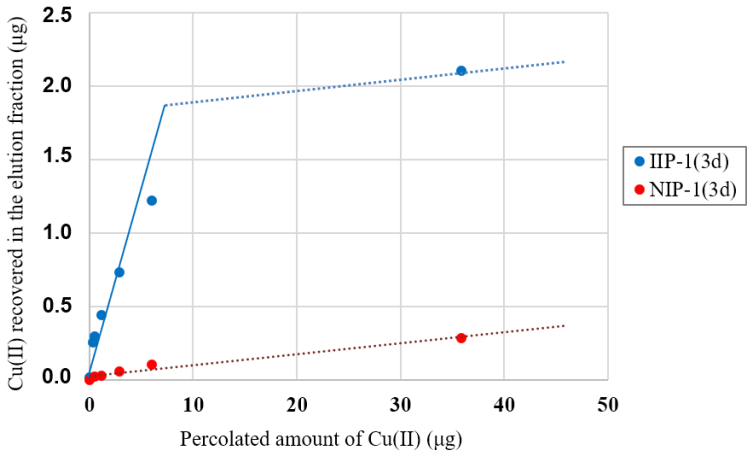

Figure 3. Adsorption capacity curves obtained by percolating an increasing amount of Cu(II) on IIP-1(3d) and its NIP. Amounts of Cu(II) were recovered in the elution fraction (2 mL of 5% HNO_3) after percolation of 1 mL of HNO_3 at pH 5.5 and washing with 5 mL of HNO_3 at pH 4.

On the basis of the experiment data obtained during the capacity determination (**Figure 3**), seven isotherm models were applied to further elucidate the mechanism of adsorption. Langmuir [60], Freundlich [61], Redlich–Peterson [62], Sips [63], Dubinin-Radushkevich [64], single-site Scatchard [65], and dual-site Scatchard [66] isotherm were employed for IIP-1(3d), while single-site Scatchard for NIP-1(3d). The equation of each model as well as the definition of parameters are detailed in Table S4 in Supplementary Material. The parameters calculated with each model and the obtained regression coefficients R^2 were summarized in **Table 4**, and their plots were provided in **Figure S4** in Supplementary Material.

Langmuir isotherm is basically representative of monolayer adsorption occurring on an energetically uniform surface, while the Freundlich isotherm, fundamentally more empirical, assumes a multilayer adsorption occurring onto a heterogeneous surface. By comparing the obtained R^2, the adsorption data of IIP-1(3d) seemed to fit better Freundlich than Langmuir isotherm, reflecting that the retention of Cu(II) on IIP-1(3d) was relevant more to a multilayer adsorption. Next, Redlich–Peterson isotherm is a hybrid model, reducing to Henry's law when the exponent $\beta = 0$, while reducing to Langmuir isotherm when the exponent $\beta = 1$. With IIP-1(3d), the β was obtained to be 0.67, confirming that the adsorption by IIP-1(3d) did not occur on an ideal monolayer.

Sips isotherm is another hybrid isotherm (also called Langmuir–Freundlich isotherm), approximating the Freundlich model at low concentration, while approximating Langmuir model at high concentration. With this incorporation of two models, Sips isotherm can be applied to both monolayer adsorption and multilayer adsorption. Indeed, the Sip isotherm presented the best R^2 as compared to the three above-mentioned isotherms, describing best the adsorption behavior of IIP-1(3d).

Dubinin-Radushkevich model offers a mean free energy of sorption E (kJ mol^{-1}), defined as the energy required to transfer one mole of ion from the solution to the sorbent surface. When $E < 8$ kJ mol^{-1}, the adsorption is deemed as a physical process. When E lies between 8 and 16 kJ mol^{-1}, the adsorption is deemed as a chemical process. In the case of IIP-1(3d), a quite acceptable correlation was obtained with Dubinin-Radushkevich model ($R^2 = 0.987$), leading to an E value of 12.62 kJ mol^{-1} in a good accordance with the ion-exchange process.

Scatchard (single-site) model assumes that the binding sites are homogeneous, so that it was usually used to identify if a sorbent possesses more than one kind of binding sites [67-69]. As a result, the Scatchard (single-site) model fitted much better the adsorption data of NIP-1(3d) than that of IIP-1(3d) according to their obtained R^2, i.e. 0.883 *vs.* 0.482. This seemed to confirm that NIP-1(3d) possesses only one set of binding sites causing non-specific interactions, while IIP-1(3d) possesses the specific cavities in addition to the non-specific sites, leading to two sets of binding sites. This assumption was successfully substantiated using Scatchard (dual-site) model to fit the adsorption data of IIP-1(3d). Indeed, the Scatchard (dual-site) exhibited the highest R^2 among all tested isotherms, i.e. 0.994.

Furthermore, in addition to high R^2, the maximum adsorption capacities predicted by those isotherm models were all of the same order of magnitude as the experimentally determined capacity, i.e. 63 μg g^{-1}, indicating a good applicability of those isotherm models.

Table 4. Parameters of the isotherm models for IIP-1(3d) as well as the parameters of Scatchard (single-site) model for its NIP. C_e (mg L^{-1}): equilibrium concentration of Cu(II); Q_e (mg g^{-1}): adsorption capacity at equilibrium; Q_m (mg g^{-1} unless specified otherwise): maximum adsorption capacity; K or E refers to the constant related to each model; n or β refers to the exponent related to each model. The equation of each model as well as the definition of parameters are detailed in Table S4 in Supplementary Material.

Model	Parameters			R^2
	Q_m (mg g^{-1})	Constant (K or E)	Exponent (n or β)	
Langmuir	0.08	0.25	/	0.960
Freundlich	/	0.02 $L^{1/n}$ $mg^{1-1/n}$ g^{-1}	2.74	0.981
Redlich–Peterson	/	K_1: 10.30 L g^{-1} K_2: 0.23 L mg^{-1}	0.67	0.982
Sips	0.14	0.17 L mg^{-1}	1.90	0.986
Dubinin-Radushkevich	3.33 x 10^{-6} mol g^{-1}	12.62 kJ mol^{-1}	/	0.987
Scatchard (single-site)	0.02	10.52	/	0.482
	5.10 x 10^{-4}	1.81	/	0.883(NIP)
Scatchard (dual-site)	$Q_{m,1}$: 0.009 $Q_{m,2}$: 0.074	K_1: 33.26 K_2: 0.15	/	0.994

3.6 Application of IIP-1(3d) with real samples

Prior to the application with real samples, the preconcentration performance of IIP-1(3d) was investigated by increasing the percolation volume up to 50 mL, first with a pure media, i. e. an HNO_3 solution at pH 5.5 spiked with Cu(II) at 2.3 µg L^{-1}. In this case, the total amount of Cu(II) introduced was 115 ng, largely inferior to the previously determined capacity of IIP-1(3d), i.e. 1.4 µg of Cu(II) for 30 mg of sorbent. After applying the optimum washing step (i.e. 5 mL of HNO_3 at pH 4), recoveries of Cu(II) on IIP-1(3d) and its NIP in the elution fraction (i.e. 2 mL of 5% HNO_3) were found to be 97% and 13%, respectively. Thus, an enrichment factor of 24 was achieved with the IIP-1(3d) and a volume of 50 mL can be percolated on 30 mg of sorbent without reaching the breakthrough volume.

Then, real samples were tested to evaluate the potential of IIP-1(3d) as well as of the developed SPE protocol for the determination of Cu(II) in complex matrices. First, 50 mL of two mineral waters, Evian® and Mont Roucous®, were tested without addition of Cu(II), which led to the determination of the initial amount of Cu(II): 0.20 ± 0.01 µg L^{-1} in Mont Roucous®, and 0.09 ± 0.01 µg L^{-1} in Evian®, using the extraction recovery previously measured with ultra-pure water for the same percolated volume (n=3). Next, they were accurately spiked with Cu(II) at 4 µg L^{-1}. As compared to the quantity of

Cu(II), these samples contained a huge quantity of interfering ions like Ca(II), Mg(II), Na(I), etc. Their contents as well as the calculated quantity ratio to the added Cu(II) are provided in **Table S5** in Supplementary Material. For example, in the case of the Evian® mineral water, the quantity of Ca(II) can be 2 x 10^4 times higher than that of Cu(II). Then, 50 mL of each spiked sample were percolated and, after washing, the proposed SPE protocol resulted in satisfactory recoveries for both mineral waters (**Table 5**). The predetermined enrichment factor was also achieved.

Finally, a seawater sample was tested. The initial content of Cu(II) was determined to be 1.79 ± 0.16 µg L^{-1}. Next, 50 mL of the non-spiked sample was tested, but unfortunately resulted in a bad recovery of Cu(II) likely due to the extremely complex matrix present herein. Indeed, the sea water presented a salinity between 31.6 and 32.6 g kg^{-1} (see Figure S5 in Supplementary Date) wherein the content of Na(I) reached normally up to 10 g L^{-1}, namely more than 5 x 10^6 times higher than the above-mentioned concentration of Cu(II). In addition, natural organic matters present in the sea water may reduce the retention of Cu(II) in a similar manner as the impact of Bis-Tris buffer shown in the section 3.2. The final SPE protocol was carried out with the percolated volume reduced to 1 mL of sea water. The sea water was tested by spiking with Cu(II) at different concentrations. After washing, the elution was performed with only 1 mL of 5% HNO_3 to avoid the dilution of Cu(II). As a result, the determination of Cu(II) was successfully performed showing quite good and repeatable recoveries for all the tests with the sea water (**Table 5**). Moreover, these recoveries were somewhat lower than those obtained with mineral waters, which seems to confirm the presence of matrix effect with the sea water.

In summary, these results demonstrated a noticeably high tolerance of IIP-1(3d) to interfering ions for the selective extraction of Cu(II). Additionally, the developed SPE protocol appeared highly suitable for the preconcentration and/or determination of Cu(II) from different and complex samples.

Table 5. Extraction recoveries of Cu(II) from natural water samples with 30 mg of IIP-1(3d) (n = 3). Results are given as mean ± standard deviation of three replicate tests. Percolation: 50 mL of spiked mineral water or 1 mL of sea water adjusted at pH 5.5; Washing: 5 mL of HNO_3 at pH 4.0; Elution: 2 mL of 5% HNO_3 for mineral water, and 1 mL of 5% HNO_3 for sea water.

Sample	Cu(II) initially present	Cu(II) added (µg L^{-1})	Cu(II) found (µg L^{-1})	Extraction recovery (%)

	($\mu g\ L^{-1}$)			
Mineral water (Mont Roucous®)	0.20 ± 0.01	4	3.93 ± 0.13	94 ± 3%
Mineral water (Evian®)	0.09 ± 0.01	4	3.79 ± 0.07	93 ± 2%
Sea water	1.79 ± 0.16	2	2.85 ± 0.16	75 ± 4%
		4	4.38 ± 0.32	76 ± 6%
		6	6.32 ± 0.69	81 ± 9%

The reusability and stability of IIP-1(3d) were assessed. As a matter of fact, the same SPE cartridge of IIP-1(3d) was utilized throughout this work from the selectivity and specificity study at the beginning, to the capacity determination, and finally to the successful application to different real samples. To sum up, more than 50 SPE procedures were carried out during almost two years, and about the last 20 of them were performed with real water samples showing high and repeatable recoveries. That demonstrated a high reusability as well as an excellent stability of the IIP-1(3d), which may be attributed to the highly cross-linked and rigid structure produced by the synthesis conditions, in particular the template/monomer/cross-linker ratio and bulk polymerization technique. Furthermore, this is very advantageous for using IIP in SPE since the ease of reuse is one of its advantages over dSPE.

4 Conclusions

Several Cu-IIPs were synthesized in methanol or ACN with Cu(II), MAA, and EGDMA as template ion, functional monomer, and crosslinking agent, respectively. Their characterization was carried out in SPE, but unlike other reported works, an optimized washing step was involved before the elution of target ions Cu(II). The washing condition was finely optimized by tuning the pH and volume of solution, allowing to eliminate the interfering ions retained by non-specific interactions without affecting the Cu(II) retained in specific cavities. The proposed methodology is actually a generic way to maximize the selective extraction performance of an IIP.

In this work, ACN was found to be a better porogen solvent than methanol as the resultant IIP showed a better specificity to Cu(II) in the presence of interfering ions. The repeatability of synthesis and of SPE results were demonstrated. However, regarding selectivity, it seemed that the acid treatment impacts strongly the properties of a NIP, particularly the porosity, revealing for the first time that the post-treatment of NIP after its polymerization should be specified. Moreover, an IIP synthesized with a different

element to Cu(II) might be considered as a better alternative control polymer to NIP. It was also clearly demonstrated that the selectivity was improved by extending the time of complexation between the template ion and the monomer. The capacity of the best IIP was determined to be 63 μg g^{-1}, and its adsorption behavior was well elucidated using several different isotherm models. Finally, applications to mineral and sea waters were successfully performed, demonstrating the high potential of the IIP and the developed SPE protocol for different and complex samples.

Acknowledgments

This work was supported by the French Research Institute for Exploitation of the Sea (Ifremer) as well as the SURIMI project funded by the Agence Nationale de la Recherche (ANR-18-CE04-0010). The authors gratefully acknowledge the Soft Matter Science and Engineering Laboratory (SIMM) of ESPCI Paris for thermogravimetric analyses and the Institute of Porous MAterials of Paris (IMAP, a joint CNRS-ENS-ESPCI laboratory) for BET experiments.

References

[1] M. Olivares, M. Araya, R. Uauy, Copper Homeostasis in Infant Nutrition: Deficit and Excess, J. Pediatr. Gastroenterol. Nutr. 31(2) (2000) 102-111.

[2] E.D. Harris, Basic and Clinical Aspects of Copper, Crit. Rev. Clin. Lab. Sci. 40(5) (2010) 547-586. https://doi.org/10.1080/10408360390250649

[3] F.M. Morel, N.M. Price, The biogeochemical cycles of trace metals in the oceans, Science 300(5621) (2003) 944-7. https://doi.org/10.1126/science.1083545

[4] I. Dakova, I. Karadjova, I. Ivanov, V. Georgieva, B. Evtimova, G. Georgiev, Solid phase selective separation and preconcentration of Cu(II) by Cu(II)-imprinted polymethacrylic microbeads, Anal. Chim. Acta 584(1) (2007) 196-203. https://doi.org/10.1016/j.aca.2006.10.050

[5] L.A. Malik, A. Bashir, A. Qureashi, A.H. Pandith, Detection and removal of heavy metal ions: a review, Environ. Chem. Lett. 17(4) (2019) 1495-1521. https://doi.org/10.1007/s10311-019-00891-z

[6] H. Nishide, E. Tsuchida, Selective adsorption of metal ions on poly(4-vinylpyridine) resins in which the ligand chain is immobilized by crosslinking, Makromol. Chem. 177 (1976).

[7] E. Ghorbani-Kalhor, M. Behbahani, J. Abolhasani, Application of Ion-Imprinted Polymer Nanoparticles for Selective Trace Determination of Palladium Ions in Food and Environmental Samples with the Aid of Experimental Design Methodology, Food Anal. Methods. 8(7) (2015) 1746-1757. https://doi.org/10.1007/s12161-014-0057-7

[8] F. Fereidoonipour, H.R. Rajabi, Development of flow injection analysis-solid phase extraction based on ion imprinted polymeric nanoparticles as an efficient and selective technique for preconcentration of zinc ions from aqueous solution, New J. Chem. 41(17) (2017) 8828-8836. https://doi.org/10.1039/c7nj00893g

[9] M. Moussa, V. Pichon, C. Mariet, T. Vercouter, N. Delaunay, Potential of ion imprinted polymers synthesized by trapping approach for selective solid phase extraction of lanthanides, Talanta 161 (2016) 459-468. https://doi.org/10.1016/j.talanta.2016.08.069

[10] H. Faghihian, Z. Adibmehr, Comparative performance of novel magnetic ion-imprinted adsorbents employed for Cd2+, Cu2+ and Ni2+ removal from aqueous solutions, Environ. Sci. Pollut. Res. 25(15) (2018) 15068-15079. https://doi.org/10.1007/s11356-018-1732-9

[11] Q.O. Dos Santos, M.A. Bezerra, G. De Fátima Lima, K.M. Diniz, M.G. Segatelli, T.O. Germiniano, V. Da Silva Santos, C.R.T. Tarley, Synthesis, characterization and application of ion imprinted poly(vinylimidazole) for zinc ion extraction/preconcentration with faas determination, Quim. Nova 37(1) (2014) 63-68. https://doi.org/10.1590/S0100-40422014000100012

[12] N. Ashouri, A. Mohammadi, M. Shekarchi, R. Hajiaghaee, H. Rastegar, Synthesis of a new ion-imprinted polymer and its characterization for the selective extraction and determination of nickel ions in aqueous solutions, Desalin. Water Treat. 56(8) (2015) 2135-2144. https://doi.org/10.1080/19443994.2014.960469

[13] K. Laatikainen, D. Udomsap, H. Siren, H. Brisset, T. Sainio, C. Branger, Effect of template ion-ligand complex stoichiometry on selectivity of ion-imprinted polymers, Talanta 134 (2015) 538-545. https://doi.org/10.1016/j.talanta.2014.11.050

[14] T. Zhang, X. Yue, K. Zhang, F. Zhao, Y. Wang, K. Zhang, Synthesis of Cu(II) ion-imprinted polymers as solid phase adsorbents for deep removal of copper from concentrated zinc sulfate solution, Hydrometallurgy 169 (2017) 599-606. https://doi.org/10.1016/j.hydromet.2017.04.005

[15] N. Guo, S.J. Su, B. Liao, S.L. Ding, W.Y. Sun, Preparation and properties of a novel macro porous Ni2+-imprinted chitosan foam adsorbents for adsorption of nickel ions from aqueous solution, Carbohydrate Polymers 165 (2017) 376-383. https://doi.org/10.1016/j.carbpol.2017.02.056

[16] Y. El Ouardi, A. Giove, M. Laatikainen, C. Branger, K. Laatikainen, Benefit of ion imprinting technique in solid-phase extraction of heavy metals, special focus on the last decade, J. Environ. Chem. Eng. 9(6) (2021). https://doi.org/10.1016/j.jece.2021.106548

[17] C. Cui, M. He, B. Chen, B. Hu, Restricted accessed material-copper(II) ion imprinted polymer solid phase extraction combined with inductively coupled plasma-optical emission spectrometry for the determination of free Cu(II) in urine and serum samples, Talanta 116 (2013) 1040-6. https://doi.org/10.1016/j.talanta.2013.08.027
[18] N.T. Hoai, D. Kim, Synthesis, structure, and selective separation behavior of copper-imprinted microporous polymethacrylate beads, AIChE J. 55(12) (2009) 3248-3254. https://doi.org/10.1002/aic.11943
[19] N.T. Hoai, D.K. Yoo, D. Kim, Batch and column separation characteristics of copper-imprinted porous polymer micro-beads synthesized by a direct imprinting method, J. Hazard. Mater. 173(1-3) (2010) 462-7. https://doi.org/10.1016/j.jhazmat.2009.08.107
[20] V. Yilmaz, O. Hazer, S. Kartal, Synthesis, characterization and application of a novel ion-imprinted polymer for selective solid phase extraction of copper(II) ions from high salt matrices prior to its determination by FAAS, Talanta 116 (2013) 322-9. https://doi.org/10.1016/j.talanta.2013.05.047
[21] V. Yilmaz, Z. Arslan, O. Hazer, H. Yilmaz, Selective solid phase extraction of copper using a new Cu(II)-imprinted polymer and determination by inductively coupled plasma optical emission spectroscopy (ICP-OES), Microchem. J. 114 (2014) 65-72. https://doi.org/10.1016/j.microc.2013.12.002
[22] S. Brunauer, P.H. Emmett, E. Teller, Adsorption of Gases in Multimolecular Layers, J. Am. Chem. Soc. 60(2) (1938) 309-319. https://doi.org/10.1021/ja01269a023
[23] S. Blain, J. Guillou, P. Treguer, P. Woerther, L. Delauney, E. Follenfant, O. Gontier, M. Hamon, B. Leilde, A. Masson, C. Tartu, R. Vuillemin, High frequency monitoring of the coastal marine environment using the MAREL buoy, Environ. Monit. Assess. 6(6) (2004) 569-75. https://doi.org/10.1039/b314073c
[24] M. Roushani, S. Abbasi, H. Khani, Synthesis and application of ion-imprinted polymer nanoparticles for the extraction and preconcentration of copper ions in environmental water samples, Environ. Monit. Assess. 187(4) (2015) 219. https://doi.org/10.1007/s10661-015-4468-8
[25] Y. Jiang, D. Kim, Effect of solvent/monomer feed ratio on the structure and adsorption properties of Cu2+-imprinted microporous polymer particles, J. Chem. Eng. 166(1) (2011) 435-444. https://doi.org/10.1016/j.cej.2010.11.006
[26] S. Mishra, A. Tripathi, Selective solid phase extraction and pre-concentration of Cu(II) ions from aqueous solution using Cu(II)-ion imprinted polymeric beads, J. Environ. Chem. Eng. 8(2) (2020) 103656. https://doi.org/10.1016/j.jece.2020.103656
[27] M. Moussa, M.M. Ndiaye, T. Pinta, V. Pichon, T. Vercouter, N. Delaunay, Selective solid phase extraction of lanthanides from tap and river waters with ion imprinted polymers, Anal. Chim. Acta 963 (2017) 44-52. https://doi.org/10.1016/j.aca.2017.02.012
[28] H. Faghihian, F.G. Adivi, Separation and pre-concentration of Cu(II) ions by a synthesized ion-imprinted polymer, Adsorption Sci. Technol. 30(3) (2012) 205-215. https://doi.org/10.1260/0263-6174.30.3.205
[29] H. Xu, D. Guo, Synthesis and characterization of an ion-imprinted polymer for selective adsorption of copper ions in aqueous solution, Adsorption Sci. Technol. 30(4) (2012) 293-306. https://doi.org/10.1260/0263-6174.30.4.293
[30] F. Shakerian, K.H. Kim, E. Kwon, J.E. Szulejko, P. Kumar, S. Dadfarnia, A.M. Haji Shabani, Advanced polymeric materials: Synthesis and analytical application of ion imprinted polymers as selective sorbents for solid phase extraction of metal ions, TrAC Trends Anal. Chem. 83 (2016) 55-69. https://doi.org/10.1016/j.trac.2016.08.001
[31] J. Park, H.A. Dam, D. Kim, Selective sorption behavior of metal(II) ion-imprinted polymethacrylate microspheres synthesized via precipitation polymerization method, Korean J. Chem. Eng. 32(5) (2015) 967-973. https://doi.org/10.1007/s11814-014-0374-y
[32] Z. Liu, Z. Hu, Y. Liu, M. Meng, L. Ni, X. Meng, G. Zhong, F. Liu, Y. Gao, Monodisperse magnetic ion imprinted polymeric microparticles prepared by RAFT polymerization based on γ-

Fe2O3@meso-SiO2nanospheres for selective solid-phase extraction of Cu(ii) in water samples, RSC Adv. 5(65) (2015) 52369-52381. https://doi.org/10.1039/c5ra07022h
[33] F.A.C. Suquila, L.L.G. de Oliveira, C.R.T. Tarley, Restricted access copper imprinted poly(allylthiourea): The role of hydroxyethyl methacrylate (HEMA) and bovine serum albumin (BSA) on the sorptive performance of imprinted polymer, J. Chem. Eng. 350 (2018) 714-728. https://doi.org/10.1016/j.cej.2018.05.176
[34] C.M.H. Ferreira, I.S.S. Pinto, E.V. Soares, H.M.V.M. Soares, (Un)suitability of the use of pH buffers in biological, biochemical and environmental studies and their interaction with metal ions – a review, RSC Adv. 5(39) (2015) 30989-31003. https://doi.org/10.1039/c4ra15453c
[35] E. Demirbas, N. Dizge, M.T. Sulak, M. Kobya, Adsorption kinetics and equilibrium of copper from aqueous solutions using hazelnut shell activated carbon, J. Chem. Eng. 148(2-3) (2009) 480-487. https://doi.org/10.1016/j.cej.2008.09.027
[36] R.D. Shannon, Revised Effective Ionic Radii and Systematic Studies of Interatomie Distances in Halides and Chaleogenides, Acta Cryst. A32 (1976) 751.
[37] C. Baggiani, F. Trotta, G. Giraudi, G. Moraglio, A. Vanni, Chromatographic characterization of a molecularly imprinted polymer binding theophylline in aqueous buffers, J. Chromatogr. A 786(1) (1997) 23-29. https://doi.org/10.1016/S0021-9673(97)00537-2
[38] B. Sellergren, K.J. Shea, Chiral ion-exchange chromatography. Correlation between solute retention and a theoretical ion-exchange model using imprinted polymers, J. Chromatogr. A 654(1) (1993) 17-28. https://doi.org/10.1016/0021-9673(93)83061-v
[39] H. Irving, R.J.P. William, The Stubility of Transition-metal Complexes, J. Chem. Soc. (1953) 3192-3210.
[40] M. Kim, Y. Jiang, D. Kim, Zn2+-imprinted porous polymer beads: Synthesis, structure, and selective adsorption behavior for template ion, React. Funct. Polym. 73(6) (2013) 821-827. https://doi.org/10.1016/j.reactfunctpolym.2013.03.012
[41] M.C. Burleigh, S. Dai, E.W. Hagaman, J.S. Lin, Imprinted Polysilsesquioxanes for the Enhanced Recognition of Metal Ions, Chemistry of Materials 13(8) (2001) 2537-2546. https://doi.org/10.1021/cm000894m
[42] H. He, Q. Gan, C. Feng, Synthesis and characterization of a surface imprinting silica gel polymer functionalized with phosphonic acid groups for selective adsorption of Fe(III) from aqueous solution, J. Appl. Polym. Sci. 134(36) (2017). https://doi.org/10.1002/app.45165
[43] M. Roushani, T.M. Beygi, Z. Saedi, Synthesis and application of ion-imprinted polymer for extraction and pre-concentration of iron ions in environmental water and food samples, Spectrochim. Acta, Part A 153 (2016) 637-44. https://doi.org/10.1016/j.saa.2015.09.029
[44] F.A.C. Suquila, L.L.G. de Oliveira, C.R.T. Tarley, Copper imprinted poly(allylthiourea): The role of hydroxyethyl methacrylate (HEMA) and bovine serum albumin (BSA) on the sorptive performance of imprinted polymer, J. Chem. Eng. 350 (2018) 714-728. https://doi.org/10.1016/j.cej.2018.05.176
[45] M. Mitreva, I. Dakova, I. Karadjova, Iron(II) ion imprinted polymer for Fe(II)/Fe(III) speciation in wine, Microchem. J. 132 (2017) 238-244. https://doi.org/10.1016/j.microc.2017.01.023
[46] S. Özkara, M. Andaç, V. Karakoç, R. Say, A. Denizli, Ion-imprinted PHEMA based monolith for the removal of Fe3+ ions from aqueous solutions, J. Appl. Polym. Sci. 120(3) (2011) 1829-1836. https://doi.org/10.1002/app.33400
[47] M. Behbahani, M. Salarian, A. Bagheri, H. Tabani, F. Omidi, A. Fakhari, Synthesis, characterization and analytical application of Zn(II)-imprinted polymer as an efficient solid-phase extraction technique for trace determination of zinc ions in food samples, J. Food Compos. Anal. 34(1) (2014) 81-89. https://doi.org/10.1016/j.jfca.2013.10.003
[48] R.L.M. Mesa, J.E.L. Villa, S. Khan, R.R.A. Peixoto, M.A. Morgano, L.M. Goncalves, M. Sotomayor, G. Picasso, Rational Design of an Ion-Imprinted Polymer for Aqueous

Methylmercury Sorption, Nanomaterials (Basel) 10(12) (2020). https://doi.org/10.3390/nano10122541
[49] F. Xie, G. Liu, F. Wu, G. Guo, G. Li, Selective adsorption and separation of trace dissolved Fe(III) from natural water samples by double template imprinted sorbent with chelating diamines, J. Chem. Eng. 183 (2012) 372-380. https://doi.org/10.1016/j.cej.2012.01.018
[50] M. Boudias, S. Korchi, A. Gourgiotis, A. Combès, C. Cazala, V. Pichon, N. Delaunay, Screening of synthesis conditions for the development of a radium ion-imprinted polymer using the dummy template imprinting approach, J. Chem. Eng. 450 (2022) 138395. https://doi.org/10.1016/j.cej.2022.138395
[51] M. Boudias, A. Gourgiotis, C. Cazala, V. Pichon, N. Delaunay, Monitoring the benefits of varying the template/monomer proportion in the synthesis of an ion-imprinted polymer for Ra(II) extraction, Advances in Sample Preparation 5 (2023). https://doi.org/10.1016/j.sampre.2022.100049
[52] F.A. Mustafai, A. Balouch, Abdullah, N. Jalbani, M.I. Bhanger, M.S. Jagirani, A. Kumar, A. Tunio, Microwave-assisted synthesis of imprinted polymer for selective removal of arsenic from drinking water by applying Taguchi statistical method, Eur. Polym. J. 109 (2018) 133-142. https://doi.org/10.1016/j.eurpolymj.2018.09.041
[53] L.D. Mafu, B.B. Mamba, T.A.M. Msagati, Synthesis and characterization of ion imprinted polymeric adsorbents for the selective recognition and removal of arsenic and selenium in wastewater samples Synthesis and characterization of ion imprinted polymeric adsorbents, J. Saudi Chem. Soc. 20(5) (2016) 594-605. https://doi.org/10.1016/j.jscs.2014.12.008
[54] B. Özkahraman, I. Acar, K. Güçlü, G. Güçlü, Synthesis of Zn(II) ion-imprinted polymeric adsorbent for selective removal of zinc from aqueous solutions, Polym.-Plast. Technol. Eng. 50(2) (2011) 216-219. https://doi.org/10.1080/03602559.2010.531434
[55] D.K. Singh, S. Mishra, Synthesis of a New Cu(II)-Ion Imprinted Polymer for Solid Phase Extraction and Preconcentration of Cu(II), Chromatographia 70(11-12) (2009) 1539-1545. https://doi.org/10.1365/s10337-009-1379-2
[56] S. Özkara, R. Say, C. Andaç, A. Denizli, An ion-imprinted monolith for in vitro removal of iron out of human plasma with beta thalassemia, Ind. Eng. Chem. Res. 47(20) (2008) 7849-7856. https://doi.org/10.1021/ie071471y
[57] G. Sharma, B. Kandasubramanian, Molecularly Imprinted Polymers for Selective Recognition and Extraction of Heavy Metal Ions and Toxic Dyes, J. Chem. Eng. Data 65(2) (2020) 396-418. https://doi.org/10.1021/acs.jced.9b00953
[58] B. Chen, L. Zhang, M. He, B. Hu, Cd (II) imprinted polymer modified silica monolithic capillary microextraction combined with inductively coupled plasma mass spectrometry for the determination of trace Cd (II) in biological samples, Spectrochim. Acta, Part B 164 (2020). https://doi.org/10.1016/j.sab.2019.105751
[59] A.C.S.A. Gomes, L.C. Costa, D.C. Brito, R.J. França, M.R.C. Marques, Development of a new ion-imprinted polymer (IIP) with Cd2+ ions based on divinylbenzene copolymers containing amidoxime groups, Polym. Bull. 77(4) (2019) 1969-1981. https://doi.org/10.1007/s00289-019-02842-8
[60] I. Langmuir, The adsorption of gases on plane surfaces of glass, mica and platinum, J. Am. Chem. Soc. 40(9) (1918) 1361-1403. https://doi.org/10.1021/ja02242a004
[61] H. Freundlich, Über die adsorption in lösungen, Zeitschrift für physikalische Chemie 57(1) (1907) 385-470.
[62] O.J. Redlich, D.L. Peterson, A useful adsorption isotherm, J. Phys. Chem. 63 (1959) 1024–1026.
[63] R. Sips, On the structure of a catalyst surface, J. Chem. Phys. 16(5) (1948) 490-495. https://doi.org/10.1063/1.1746922
[64] M.M. Dubinin, The Equation of the Characteristic Curve of Activated Charcoal, Proceedings of the USSR Academy of Sciences 55 (1947) 327-329.

[65] G. Scatchard, The attractions of proteins for small molecules and ions, Ann. N. Y. Acad. Sci. 51(4) (1949) 660-672. https://doi.org/10.1111/j.1749-6632.1949.tb27297.x
[66] A.K. Bordbar, A.A. Saboury, A.A. Moosavi-Movahedi, The shapes of Scatchard plots for systems with two sets of binding sites, Biochem. Educ. 24(3) (1996) 172-175. https://doi.org/10.1016/0307-4412(95)00122-0
[67] F.M. de Oliveira, B.F. Somera, E.S. Ribeiro, M.G. Segatelli, M.J. Santos Yabe, E. Galunin, C.R.T. Tarley, Kinetic and Isotherm Studies of Ni2+Adsorption on Poly(methacrylic acid) Synthesized through a Hierarchical Double-Imprinting Method Using a Ni2+ Ion and Cationic Surfactant as Templates, Ind. Eng. Chem. Res. 52(25) (2013) 8550-8557. https://doi.org/10.1021/ie4003624
[68] J.F. He, Q.H. Zhu, Q.Y. Deng, Investigation of imprinting parameters and their recognition nature for quinine-molecularly imprinted polymers, Spectrochim. Acta, Part A 67(5) (2007) 1297-305. https://doi.org/10.1016/j.saa.2006.09.040
[69] H.A. Feldman, Mathematical theory of complex ligand-binding systems at equilibrium: Some methods for parameter fitting, Anal. Biochem. 48(2) (1972) 317-338. https://doi.org/10.1016/0003-2697(72)90084-X

Supplementary Material

Table S1: ICP-MS acquisition and analysis parameters.

Acquisition parameters	RF power	1550 W
	Sampling depth	10.0 mm
	Plasma gas flow rate	15.0 L min^{-1}
	Auxiliary flow rate	0.90 L min^{-1}
	Carrier gas flow rate	1.05 L min^{-1}
Analysis parameters	Isotopes monitored	^{59}Co, ^{60}Ni, ^{63}Cu, and ^{66}Zn
	Mode	Collision (Helium)
	Peak pattern	1
	Integration time	0.3 s
	Number of replicates	5
	Number of sweeps	100

Table S2: LOD and LOQ of ^{59}Co, ^{60}Ni, ^{63}Cu, and ^{66}Zn in 2% HNO_3 determined by ICP-MS

Element	^{59}Co	^{60}Ni	^{63}Cu	^{66}Zn
LOQ (ng L^{-1})	1.9	47.0	50.6	216.0
LOD (ng L^{-1})	0.6	14.1	15.2	64.8

Table S3: Functional monomers and distribution coefficients (D) for Cu(II), Co(II), Ni(II), and Zn(II) of some NIPs in the literature. These NIPs were characterized in dSPE wherein a distribution coefficient (D) is used as a criterion to scale the binding capacity of IIP/NIP for a tested ion. The distribution coefficient (D) is expressed as $D = \frac{C_0 - C_e}{C_e} \times \frac{V}{M}$, where C_o and C_e are the concentrations of the ions in the initial solution and in the aqueous phase after adsorption, respectively (mg L^{-1}), V is the volume of the aqueous phase (mL), and M is the amount of polymer (g).

Ref.	Functional monomers	Distribution coefficient (mL g^{-1}) of NIP			
		Cu(II)	Co(II)	Ni(II)	Zn(II)
Mishra et al. [1]	picolinic acid and MMA	1030	552	524	427
Yilmaz et al. [2]	5-methyl-2-thiozylmethacrylamide	359	125	44	68
Birlik et al. [3]	chitosan-succinate	6347	280	163	257
Shamsipur et al. [4]	1-hydroxy-4-(prop-2'-enyloxy)-9,10-anthraquinone	1583	214	277	164
Li et al. [5]	N-isopropylacrylamide and γ-methacryloxypropyltrimethoxysilane	479	140	114	247
Singh et al. [6]	salicylic acid	951	146	173	732
Shamsipur et al. [7]	1,4-dihydroxy-9,10-anthraquinone	4025	248	258	280
Shah et al. [8]	2,2'-bipyridine and 4-vinylpyridine	6.8×10^{-3}	1.7×10^{-3}	2.1×10^{-3}	3.5×10^{-3}

[1] S. Mishra, A. Tripathi, Selective solid phase extraction and pre-concentration of Cu(II) ions from aqueous solution using Cu(II)-ion imprinted polymeric beads, Journal of Environmental Chemical Engineering 8(2) (2020) 103656.
[2] V. Yilmaz, O. Hazer, S. Kartal, Synthesis, characterization and application of a novel ion-imprinted polymer for selective solid phase extraction of copper(II) ions from high salt matrices prior to its determination by FAAS, Talanta 116 (2013) 322-9.
[3] E. Birlik, A. Ersöz, A. Denizli, R. Say, Preconcentration of copper using double-imprinted polymer via solid phase extraction, Analytica Chimica Acta 565(2) (2006) 145-151.
[4] M. Shamsipur, A. Besharati-Seidani, J. Fasihi, H. Sharghi, Synthesis and characterization of novel ion-imprinted polymeric nanoparticles for very fast and highly selective recognition of copper(II) ions, Talanta 83(2) (2010) 674-81.
[5] Z. Li, Q. Su, W. Jiang, L. Wu, Preparation of a thermosensitive surface imprinted polymer based on palygorskite for removal of copper (II) from environment aqueous solution, International Journal of Environmental Analytical Chemistry (2021) 1-16.
[6] D.K. Singh, S. Mishra, Synthesis of a New Cu(II)-Ion Imprinted Polymer for Solid Phase Extraction and Preconcentration of Cu(II), Chromatographia 70(11-12) (2009) 1539-1545.
[7] M. Shamsipur, A. Besharati-Seidani, Synthesis of a novel nanostructured ion-imprinted polymer for very fast and highly selective recognition of copper(II) ions in aqueous media, Reactive and Functional Polymers 71(2) (2011) 131-139.
[8] S. Jasmin, M.R. Jan, Anjum, Selective Solid Phase Extraction of Copper from Different Samples using Copper Ion-Imprinted Polymer, Journal of Analytical Chemistry 73(12) (2018) 1146-1153.

Table S4: Equations and parameters of the isotherm models for IIP-1(3d) as well as the parameters of Scatchard model for its NIP. C_e (mg L^{-1}): equilibrium concentration of Cu(II); Q_e: adsorption capacity at equilibrium; Q_m (mg g^{-1}): maximum adsorption capacity.

Model	Equation	Parameter definition
Langmuir	$Q_e = Q_m K C_e/(1 + K C_e)$	P_1: Q_m (mg g^{-1}); P_2: K, Langmuir constant related to binding affinity.
Freundlich	$Q_e = K C_e^{1/n}$	P_1: K ($L^{1/n}$ $mg^{1-1/n}$ g^{-1}), Freundlich constant related to the adsorption capacity; P_2: n, indicative parameter related to the adsorption intensity.
Redlich–Peterson	$Q_e = K_1 C_e/(1 + K_2 C_e^{\beta})$	P_1: K_1 (L g^{-1}), a Redlich–Peterson constant; P_2: K_2 (L mg^{-1}), a Redlich–Peterson constant; P_3: β, an exponent that lies between 0 and 1.
Sips	$Q_e = Q_m K C_e^{1/n}/(1 + K C_e^{1/n})$	P_1: Q_m (mg g^{-1}); P_2: K (L mg^{-1}), Sips constant; P_3: n, Sips model exponent.
Dubinin-Radushkevich	$Q_e = Q_m \exp\left(\frac{\left(RTln(1 + 1/C_e)\right)^2}{-2E^2}\right)$	P_1: Q_m (mol g^{-1}); P_2: E (kJ mol^{-1}), adsorption energy; R (8.314 J (mol K)$^{-1}$), universal gas constant; T (K), Kelvin temperature.
Scatchard (single-site)	$Q_e = \frac{Q_m K C_e}{1 + K C_e}$	P_1: Q_m (mg g^{-1}); P_2: K, a constant related to the equilibrium dissociation;
Scatchard (dual-site)	$Q_e = \frac{Q_{m,1} K_1 C_e}{1 + K_1 C_e} + \frac{Q_{m,2} K_2 C_e}{1 + K_2 C_e}$	P_1: $Q_{m,1}$ (mg g^{-1}); P_2: $Q_{m,2}$ (mg g^{-1}); $P_{3,4}$: $K_{1,2}$, constants related to the equilibrium dissociation;

Table S5: Contents (mg L^{-1}) of main ions in the mineral waters of Evian® and Mont Roucous® as well as the calculated quantity ratio to the added Cu(II) at 4.0 µg L^{-1}. The data were obtained from the labels of their bottles. Note: The dot (.) separates decimals and the comma (,) separates thousands.

Mineral water	Main ion	Content (mg L^{-1})	Quantity ratio to the added Cu(II) (4 µg L^{-1})
Evian®	Ca^{2+}	80	20,000
	Na^{+}	6.5	1,625
	Mg^{2+}	26	650
	K^{+}	1	250
	HCO_3^{-}	360	90,000
	SO_4^{2-}	14	3,500
	Cl^{-}	10	2,500
	NO_3^{-}	3.8	950
Mont Roucous®	Ca^{2+}	2.9	725
	Na^{+}	3.0	750
	Mg^{2+}	0.5	125
	SO_4^{2-}	3.0	750
	NO_3^{-}	2.0	500
	F^{-}	< 0.1	< 25

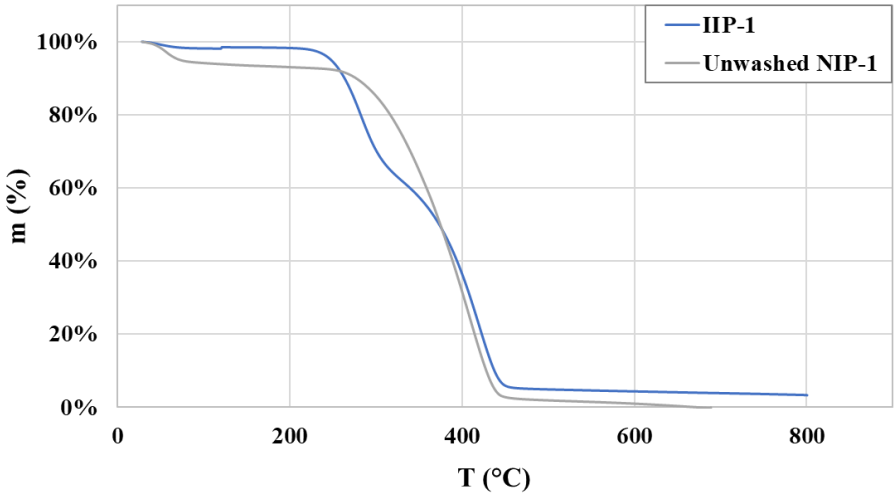

Figure S1: Thermogravimetric analyses of IIP-1 (30 mg) and unwashed NIP-1 (30 mg) performed with a scanning range of 10 – 800 °C at 10 °C min^{-1} under nitrogen gas.

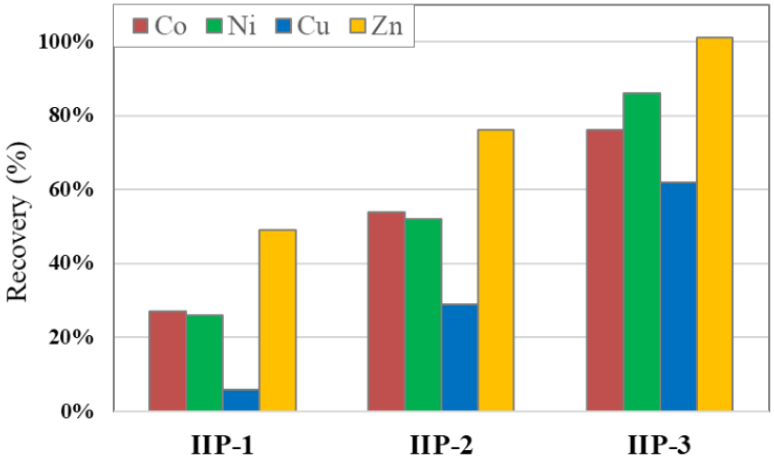

Figure S2: Recovery of Co(II), Ni(II), Cu(II), and Zn(II) in the percolation fraction on IIP-3, IIP-2, and IIP-1. Percolation: 1 mL of HNO_3 at pH 4.4 spiked with 40 µg L^{-1} Co(II), Ni(II), Cu(II), and Zn(II). No washing. Elution: 2 mL of 5% HNO_3.

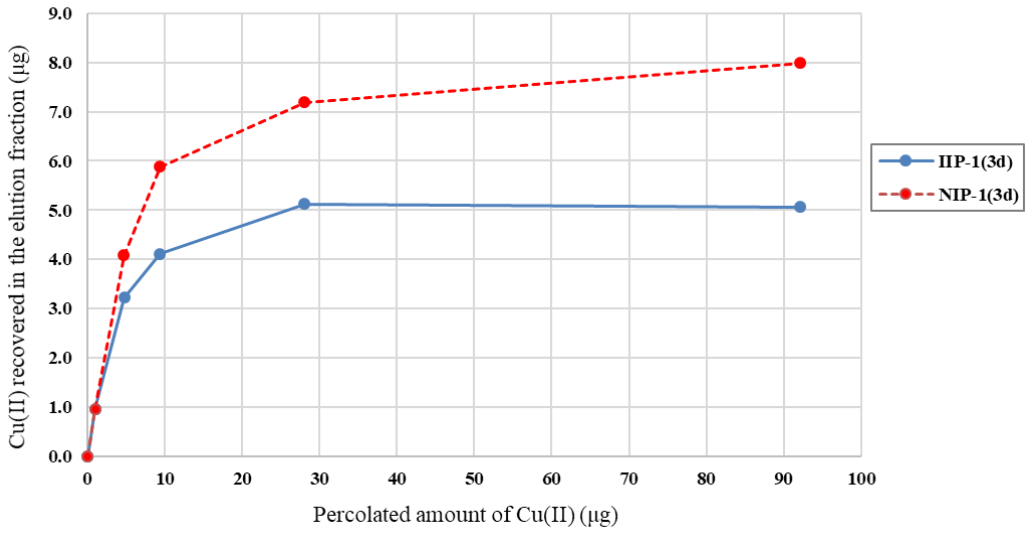

Figure S3: Adsorption capacity curves obtained by percolating an increasing amount of Cu(II) on IIP-1(3d) and its NIP. Amounts of Cu(II) were recovered in the elution fraction (2 mL of 5% HNO_3) after percolation of 1 mL of HNO_3 at pH 5.5 and without performing a washing step.

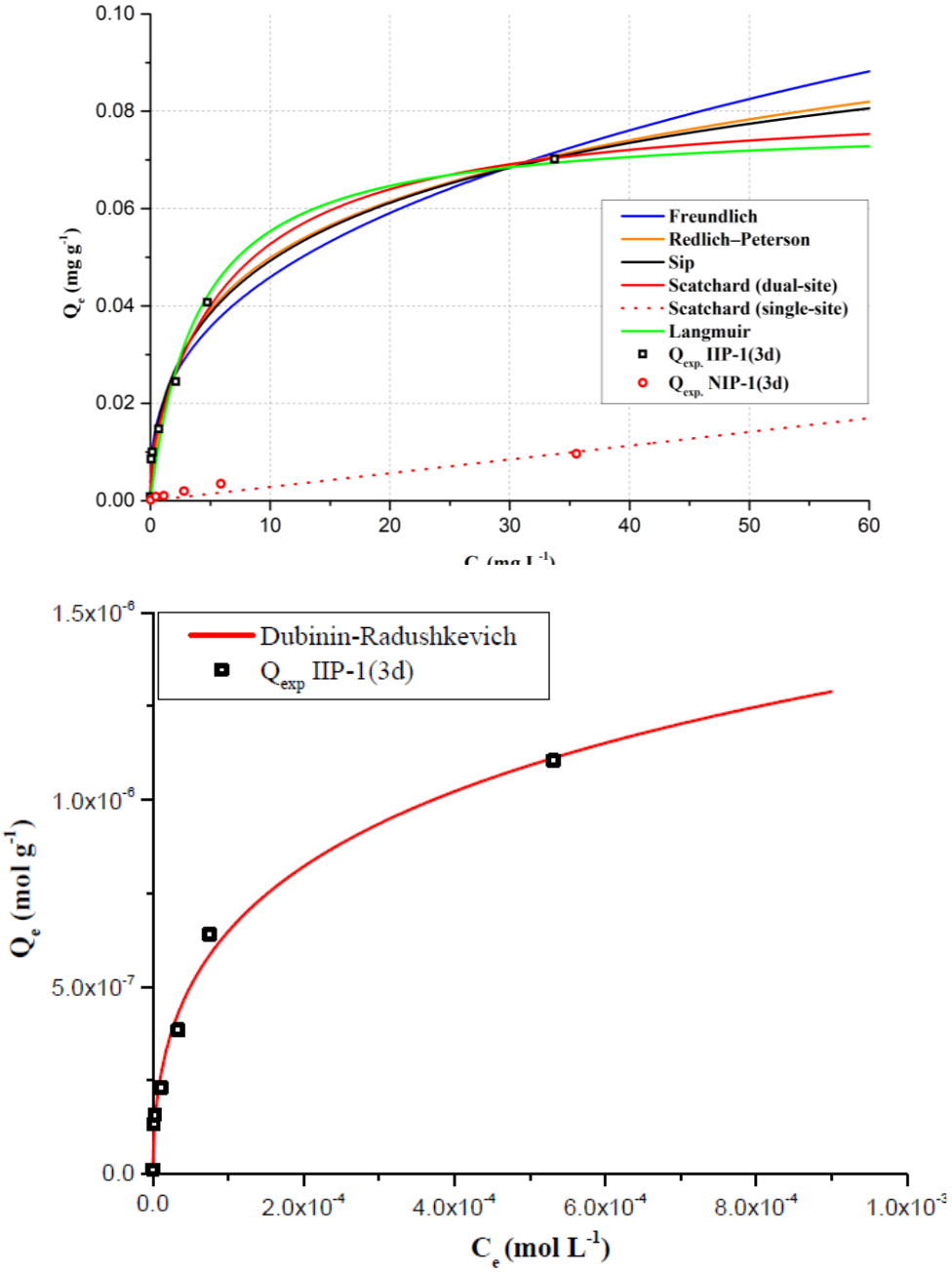

Figure S4: Plots of the isotherm models with the experimental data of IIP-1(3d) and its NIP.

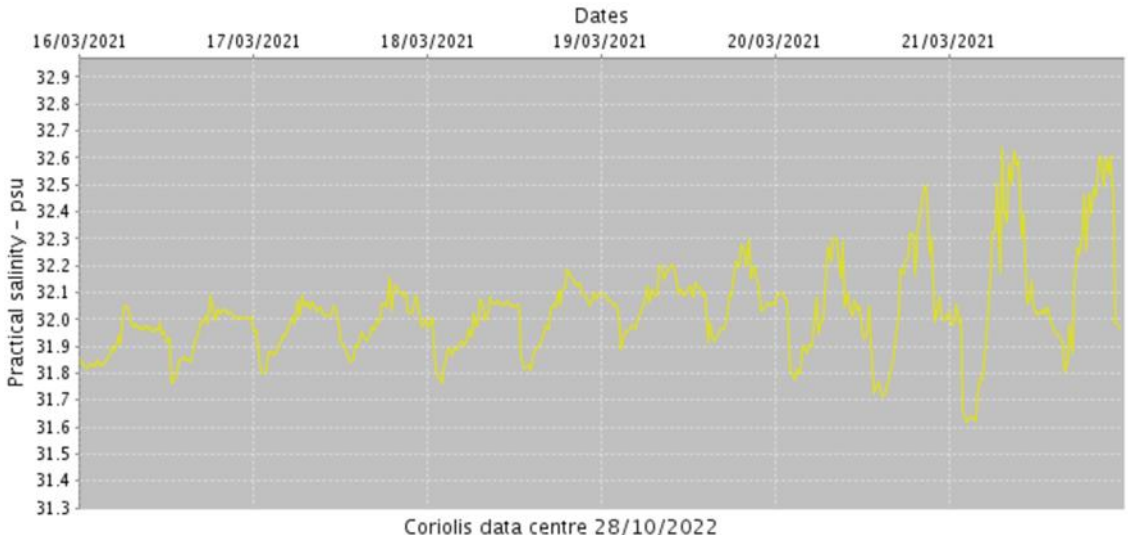

Figure S5: Measurement of the salinity of sea water using Marel Iroise buoy